ACS Pharmacology & Translational Science

pubs.acs.org/ptsci Article

Target-Driven Design of a Coumarinyl Chalcone Scaffold Based Novel EF2 Kinase Inhibitor Suppresses Breast Cancer Growth *In Vivo*

Ferah Comert Onder, Nermin Kahraman, Esen Bellur Atici, Ali Cagir, Hakan Kandemir, Gizem Tatar, Tugba Taskin Tok, Goknur Kara, Bekir Karliga, Serdar Durdagi, Mehmet Ay,* and Bulent Ozpolat*

Cite This: *ACS Pharmacol. Transl. Sci.* 2021, 4, 926–940 Read Online

ACCESS | Metrics & More | Article Recommendations | Supporting Information

ABSTRACT: Eukaryotic elongation factor 2 kinase (eEF-2K) is an unusual alpha kinase involved in protein synthesis through phosphorylation of elongation factor 2 (EF2). eEF-2K is highly overexpressed in breast cancer, and its activity is associated with significantly shortened patient survival and proven to be a potential molecular target in breast cancer. The crystal structure of eEF-2K remains unknown, and there is no potent, safe, and effective inhibitor available for clinical applications. We designed and synthesized several generations of potential inhibitors. The effect of the inhibitors at the binding pocket of eEF-2K was analyzed after developing a 3D target model by using a domain of another α-kinase called myosin heavy-chain kinase A (MHCKA) that closely resembles eEF-2K. *In silico* studies showed that compounds with a coumarin−chalcone core have high predicted binding affinities for eEF-2K. Using *in vitro* studies in highly aggressive and invasive (MDA-MB-436, MDA-MB-231, and BT20) and noninvazive (MCF-7) breast cancer cells, we identified a lead compound that was highly effective in inhibiting eEF-2K activity at submicromolar concentrations and at inhibiting cell proliferation by induction of apoptosis with no toxicity in normal breast epithelial cells. *In vivo* systemic administration of the lead compound encapsulated in single lipid-based liposomal nanoparticles twice a week significantly suppressed growth of MDA-MB-231 tumors in orthotopic breast cancer models in nude mice with no observed toxicity. In conclusion, our study provides a highly potent and *in vivo* effective novel small-molecule eEF-2K inhibitor that may be used as a molecularly targeted therapy breast cancer or other eEF-2K-dependent tumors.

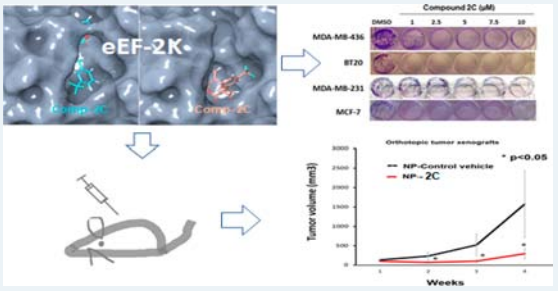

KEYWORDS: *elongation factor 2 kinase, EF2K, coumarin, molecular modeling, breast cancer, apoptosis*

Eukaryotic elongation factor 2 kinase (eEF-2K) belongs to alpha kinase family and is involved in regulation of protein synthesis by phosphorylating elongation factor 2 (EF2) as an unusual kinase.[1−3] eEF-2K has a limited sequence identity to more than 500 conventional protein kinases and cannot be inhibited by kinase inhibitors such as staurosporin. eEF-2K is activated by the calcium−calmodulin system and various oncogenic signaling, mitogen, and growth factors (i.e., EGFR). Cellular and metabolic stress such as hypoxia, nutrient-deprivation, and autophagy induce eEF-2K activity, suggesting that this kinase acts as a survival pathway.[4−10] eEF-2K plays a role in regulating the Warburg effect in tumor cells by modulating the synthesis of protein phosphatase 2A (PP2A) and promotes expression of the c-Myc pathway pyruvate kinase (PK) M2 isoform, the key glycolytic enzyme transcriptionally activated by c-Myc.[11] Recently, adenosine monophosphate-activated kinase (AMPK), one of the key regulators of energy homeostasis, was identified as another substrate of eEF-2K,[12] revealing that eEF-2K signaling is involved in regulation of the metabolism and cellular energy.

We previously demonstrated for the first time that eEF-2K is highly upregulated in triple negative breast cancer (TNBC), BRCA1-mutated, and ER$^+$ breast cancer cells, and its expression is associated with poor clinical outcome, metastatic disease, and shorter patient survival in TNBC.[13−15] Inhibition of eEF-2K by genetic methods (i.e, siRNA and miRNA) significantly suppressed cancer cell proliferation, migration, invasion, and tumorigenesis in breast cancer, pancreatic, and lung cancer models.[13−19] More importantly, *in vivo* therapeutic inhibition of eEF-2K by genetically targeted therapies using siRNA or micRNA approaches significantly suppressed growth of human cancer xenografts in various tumor models in mice, including TNBC and BRCA1-mutated breast cancers.[13,14,17,19] Furthermore, we demonstrated that *in vivo* targeting of eEF-2K by siRNA enhanced the efficacy of chemotherapy in tumor models.[13] Overall, these studies suggested that eEF-2K is an important driver of breast cancer growth, especially TNBC and

Received: January 19, 2021
Published: March 30, 2021

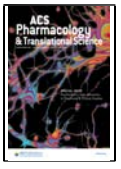

https://doi.org/10.1021/acsptsci.1c00030
ACS Pharmacol. Transl. Sci. 2021, 4, 926−940

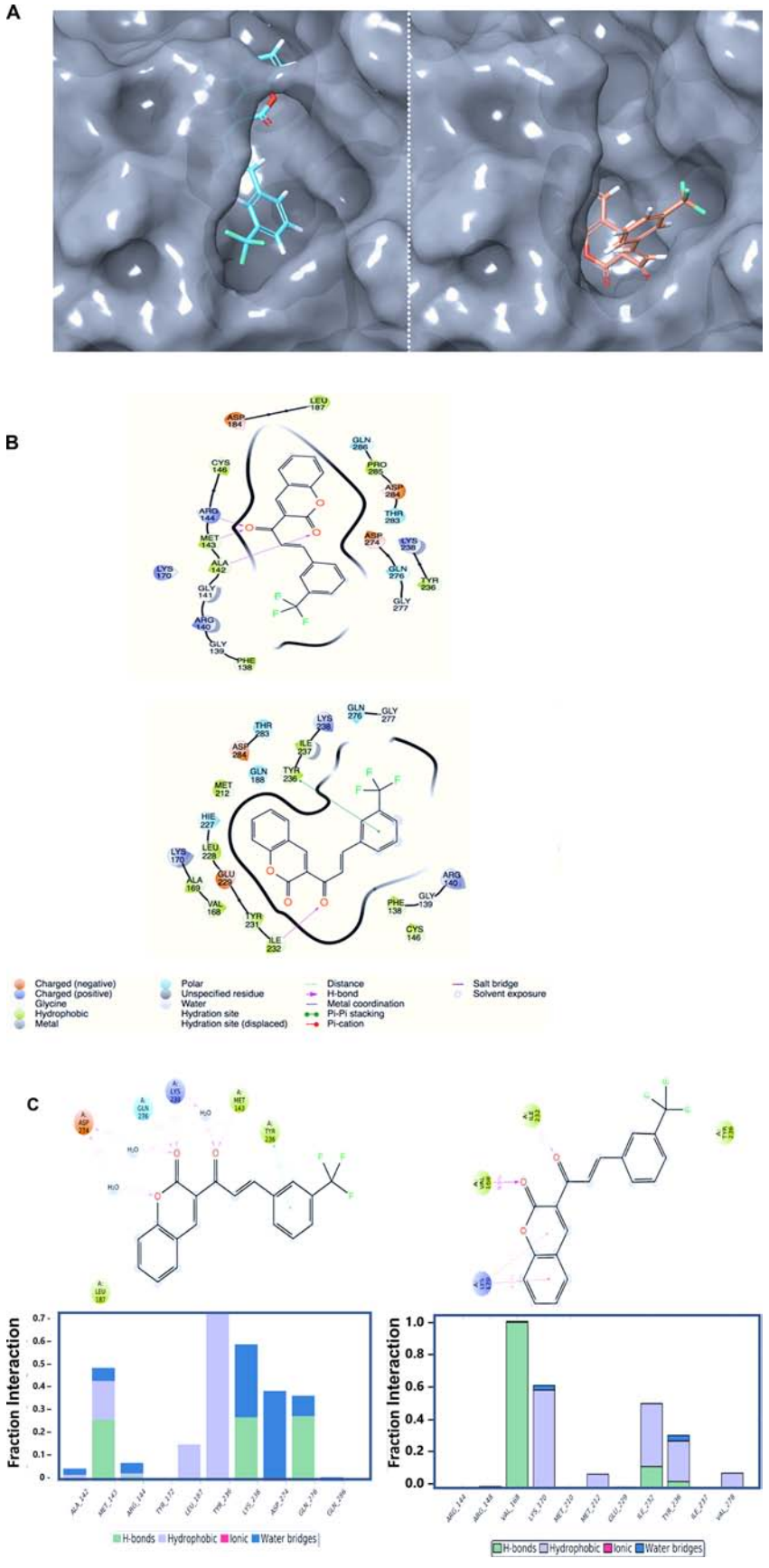

Figure 1. Docking and molecular dynamics interactions of compound **2C** and eEF-2K. (A, B) 3D and 2D ligand interactions diagram of **2C** (docking poses); (left) pose 2, (right) pose 4. (C) 2D ligand interactions diagram of **2C** (representative MD poses); (left) pose 2, (right) pose 4. The figure also shows interaction fractions of crucial residues at the binding.

https://doi.org/10.1021/acsptsci.1c00030
ACS Pharmacol. Transl. Sci. 2021, 4, 926−940

BRCA1-mutated subtypes, and serves as a potential novel molecular target breast cancers.

Development of inhibitors for effectively targeting eEF-2K have been major aim for clinical translation.[20−28] However, development of effective eEF-2K inhibitors has been highly challenging task. Several inhibitors of eEF-2K have been described in the literature.[20−28] However, these inhibitors have been neither potent nor specific for clinical applications. For instance, 1-benzyl-3-cetyl-2-methylimidazolium iodide (NH125), an imidazolium derivative, was the first inhibitor published. Studies showed that it does not inhibit eEF2 phosphorylation when exposed to cells.[29,30] Later, A-484954 (7-amino-1-cyclopropyl-3-ethyl-2,4-dioxo-1,2,3,4-tetrahydro pyrido[2,3-*d*]pyrimidine-6-carboxamide), a pyrido-pyrimidine-dione, was identified by Abbott Laboratories as eEF-2K inhibitor, but it is weak and inhibits cell proliferation at very high doses (IC_{50} ∼ 50−75 μM).[31,32] Other well-known and commercial available inhibitors, TX-1918 (2-((3,5-dimethyl-4-hydroxyphenyl)-methylene)-4-cyclopentene-1,3-dione) and DFTD (2,6-diamino-4-(2-fluorophenyl)-4*H*-triopyran-3,5-dicarbonitrile), have been reported as eEF-2K inhibitors with IC_{50} of 0.44−1 and 60 μM, respectively. However, TX-1918 has been shown to also inhibit many kinases including Src, PKA, PKC, and EGFR.[33,34] Thus, development of highly effective and selective inhibitors targeting eEF-2K is urgently needed for clinical translation.

The major obstacle for rationale drug design and development of effective eEF-2K inhibitors is the lack of information regarding its 3D structure of the catalytic domain. To overcome this challenge, we designed and screened different scaffolds of compounds and evaluated their activity by *in silico* using homology modeled target structure of eEF-2K and *in vitro* assays. Our results showed that compounds including coumarin−chalcone cores have high predicted binding affinity to eEF-2K. Thus, a series of compounds including coumarin−chalcone compounds were synthesized, and using the homology modeling, compound **2C** was identified as the lead small molecule inhibitor. Further *in silico* studies (induced fit docking -IFD, quantum polarized ligand docking, molecular dynamics (MD) simulations and postprocessing analysis of MD trajectories) were carried out and the effect of **2C** at the binding pocket of eEF-2K was investigated in atomic details. Our *in vitro* results indicated that lead inhibitor compound **2C** was highly effective in inhibiting eEF-2K in breast cancer cells at submicromolar concentrations (<1 μM) and showed significant antiproliferative effects by inducing apoptosis. More importantly, compound **2C** was also highly effective in inhibiting tumor growth of highly aggressive MDA-MB-231 tumors *in vivo* with no observed toxicity, suggesting that **2C** may be considered for *in vivo* targeting of eEF-2K and preclinical development for clinical translation.[35]

Homology Modeling, Molecular Docking, and Molecular Dynamics (MD) Simulations. Currently, the crystal structure of eEF-2K is not solved yet. However, the three-dimensional structures of the catalytic domain of another α-kinase called myosin heavy-chain kinase A (MHCKA) is available and has been studied in considerable detail.[42] Therefore, we developed a predicted model of human eEF-2K used myosin heavy-chain kinase A (MHCK-A) as a template with homology modeling studies.[47] Next, we designed and screened different scaffolds of compounds including the coumarin−chalcone scaffold and evaluated their activity by *in silico* using a homology-modeled target structure of eEF-2K. In coumarin−chalcone scaffolds, compound **2C** was identified as the lead small-molecule inhibitor. Initially, we used a rigid protein docking approach[42] with AutoDock and docking results showed that compound **2C** binds to the ATP-binding site of eEF-2K[48−49] (Figure S1). To take the flexibility of binding pocket residues of model protein into account,[47] we used the Glide/induced-fit docking (IFD) method. Glide/IFD results showed that **2C** binds to similar region identified by rigid docking; however, its binding pose was slightly different, as expected. We then used the top-docking IFD pose and carried out the long (400 ns) all-atom molecular dynamics (MD) simulations. When we checked the collected trajectories of **2C** at the binding site of the target protein, we found that compound diffuses from the binding pocket (Figure S2). Next, we used the top 5 docking poses which all have very similar docking scores changing between (−9.95 to −8.92 kcal/mol) in MD simulations. For each docking pose, 50 ns all-atom MD simulations are carried out, and MD simulations results were shown that poses 2 and 4 did not diffuse from the initial docking poses and were stable (Figure S3). Figure 1 shows 2D and 3D ligand interactions diagrams of stable docking poses of compound **2C**. In order to check the target specificity of the **2C**, we evaluated its binding to related kinases and calculated the docking scores by Glide/IFD. As mentioned above, compound **2C** which exerted a high docking score or high specific binding affinity for eEF-2K (−9.95 kcal/mol), compared to other related and clinically significant kinases, including PKC-delta (−6.43 kcal/mol), AKT-Protein kinase B (−6.39 kcal/mol), PKR-RNA-activated protein kinase (−7.58 kcal/mol), AXL (−7.11 kcal/mol), YES1 (−7.54 kcal/mol), and MAPKAP kinase 2 (MK2) (−6.67 kcal/mol) (Table S2).

Throughout the MD simulations, 1000 trajectory frames were collected, and the last 500 trajectories were used in free energy calculations of the ligand. The average molecular mechanics generalized Born surface area (MM/GBSA) predicted binding energy scores of poses 2 and 4 of compound **2C** were found to be similar (−57.88 ± 4.20 and −61.86 ± 4.30 kcal/mol, respectively). While Leu137, Met143, Tyr236, Lys238, Asp274, and Gln276 were found in crucial interactions with compound **2C** starting the MD simulations with pose 2, the corresponding residues were Val168, Lys170, Ile232, Tyr236, and Val278 when we start the MD simulations from pose 4. The main difference between poses 2 and 4 throughout the simulations were observed in solvent accessible surface area (SASA) values. Throughout the simulations initiated with pose 2, we observed water molecules that were bridging the hydrogen bonds between residues and compound **2C**.

When the induced charge polarization by the active site of the protein environment is considered, quantum mechanics (QM) modeling may give the highest level of docking accuracy. For these reasons, quantum polarized ligand docking (QPLD) is also considered which uses *ab initio* charge calculations for the docking score comparison with the previously studied eEF-2K inhibitors (Table S1). Results showed that compound **2C** (−7.691 kcal/mol) has better docking scores than some of the published eEF-2K inhibitors such as nonpotent inhibitor A484954 (−5.621 kcal/mol), NH125 (−4.503 kcal/mol), and TX-1918 (−5.533 kcal/mol), except for nonspecific eEF-2K inhibitor Rottlerin (−8.263 kcal/mol).

Pharmacological Properties and Predicted ADME Profiles of Lead Compound 2C. To determine the druglike

https://doi.org/10.1021/acsptsci.1c00030
ACS Pharmacol. Transl. Sci. 2021, 4, 926−940

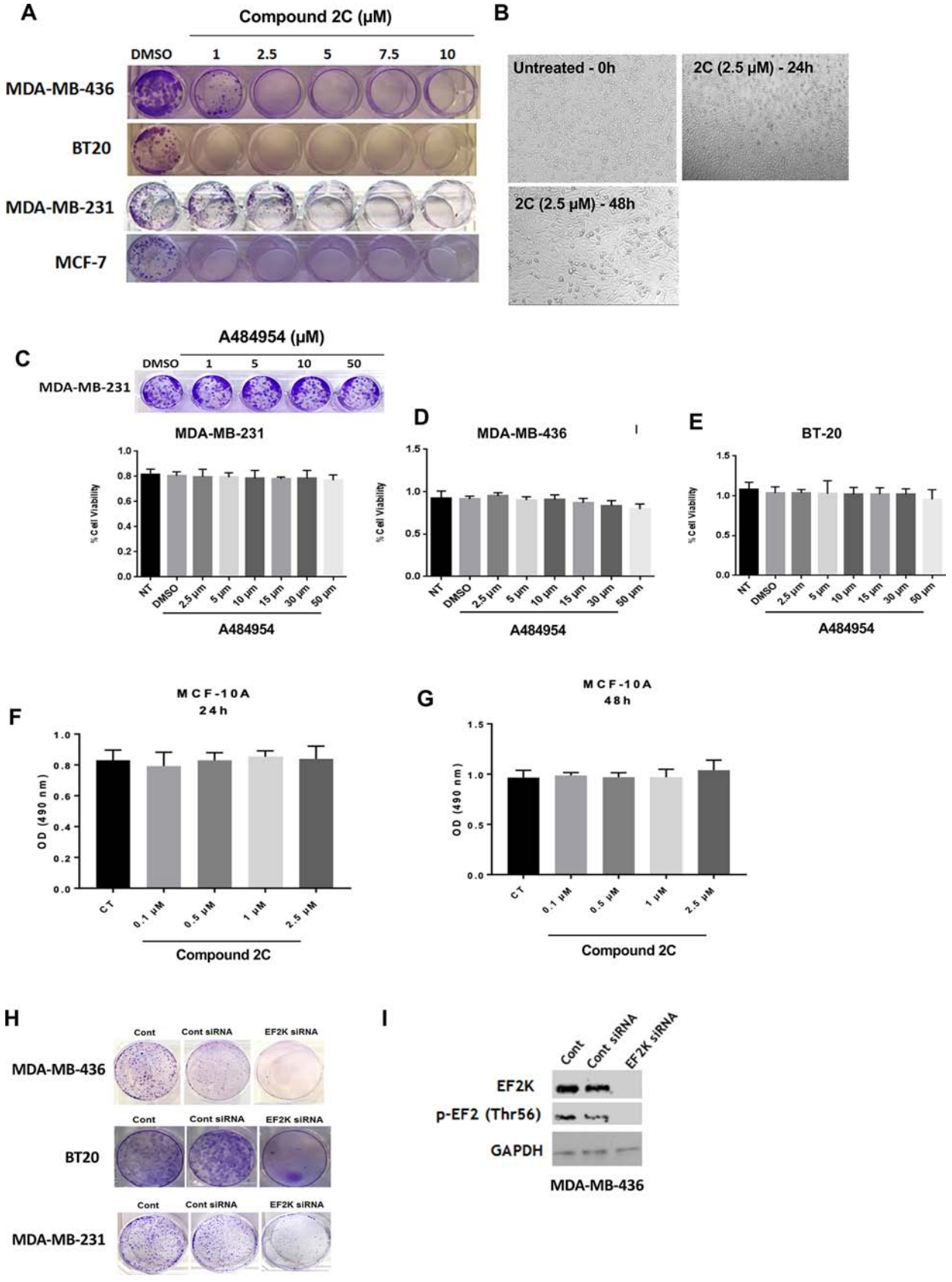

Figure 2. Compound **2C** inhibits proliferation and colony formation in breast cancer cells. (A) Effects of compound **2C** on the colony formation of highly invasive TNBC (MDA-MB-436, BT-20, and MDA-MB-231) and noninvazive ER+ MCF-7 cells. Treatment with compound **2C** led to marked inhibition of proliferation and colony formation of all BC cells in a dose-dependent manner. (B) MDA-MB-231 cells treated with **2C** cells were imaged by light microscopy at 24 and 48 h. (C–E) Treatment of BC cells with A484954, a previously reported EF2K inhibitor, did not inhibit cell proliferation up to 50 μM concentrations in the BC cells. (F, G) Compound **2C** did not show any toxicity on a normal immortalized human

https://doi.org/10.1021/acsptsci.1c00030
ACS Pharmacol. Transl. Sci. 2021, 4, 926–940

Figure 2. continued

mammary epithelial cell line for 24 and 48 h (MCF-10A). Cell colonies were stained with crystal violet, and the number of colonies was quantified after 8−14 days. (H) Knockdown of eEF-2K by a specific siRNA targeting eEF-2K mRNA suppressed cell proliferation and colony formation in MDA-MB-436, BT-20, and MDA-MB-231 cells. Cells were transfected with control or eEF-2K siRNA (50 nM) using hiperfect transfection reagent 24 h after plating cells into 6-well plates. The panels are representative images of the colony cultured 6-well plates at days 10−12. (I) eEF-2K knockdown by eEF-2K siRNA was demonstrated in MDA-MB-436 through Western blot analysis. Cells were transfected with eEF-2K or control siRNA (50 nM) and collected and analyzed 72 h later by Western blot. eEF-2K inhibition by siRNA reduced levels of both eEF-2K and its downstream substrate p-EF2 (Th56) in MDA-MB-436 cells.

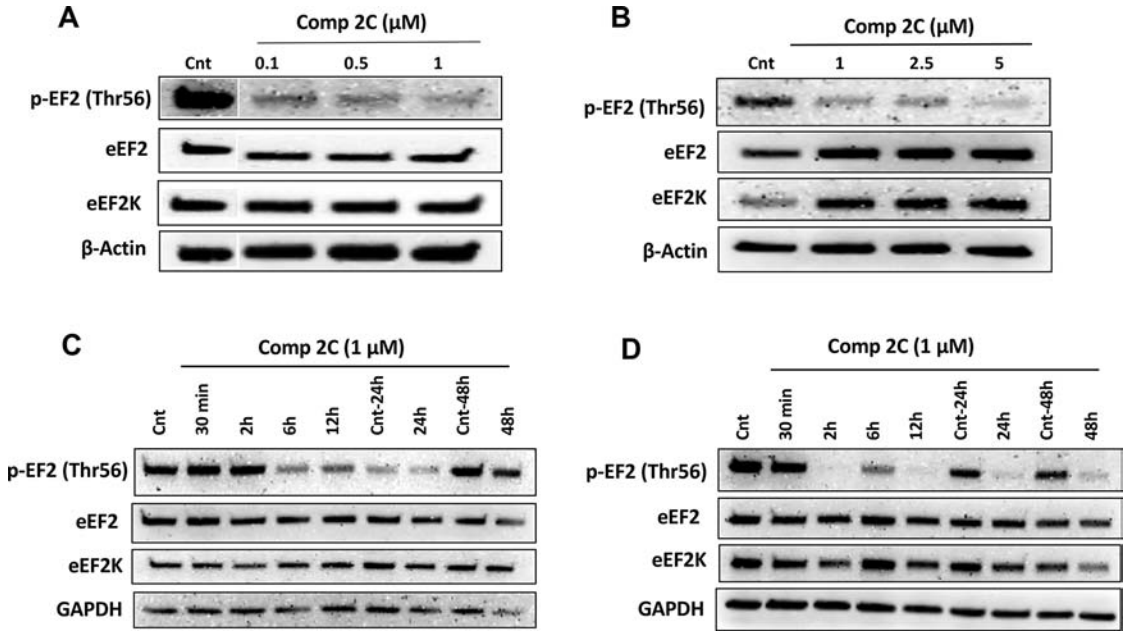

Figure 3. Compound **2C** inhibits activity of eEF-2K as indicated by reduced phosphorylation of its downstream target EF2. (A) MDA-MB-231 cells were treated with compound **2C** in the range of 0.1−1 μM and pEF2 levels analyzed by Western blot. (B) BT-20 cells were treated with increasing doses of compound **2C** (1 and 5 μM) for 6 h. (C) MDA-MB-231 cells were treated with compound **2C** between 0.1 and 1 μM for 2 h, and p-EF2 levels were evaluated. (D) MCF-7 cells were treated with compound **2C** at 1 μM up to 48 h. pEF2 levels were analyzed by Western blot.

properties of compound **2C**, we investigated pharmacokinetic properties such as blood−brain barrier (BBB, log ratio), lipophilicity, the log of compound octanol−water distribution (G-Log *P*), human serum protein binding (prot-bind, %), water solubility (WSol, log mg/L), human hERG channel inhibition (hERG-inh, pK_i), human serotonin transporter inhibition (SERT-inh, pK_i) of compound **2C**[50] (Table S3). The data for the BBB penetration model is expressed as log values of the ratio of the metabolite concentrations in brain and plasma. According to these calculations, the cutoff value of this parameter should be between −0.3 and 1.5 in the MetaCore/MetaDrug tool. Since the calculated BBB value of **2C** is very close to the cutoff value, **2C** is predicted to penetrate through the BBB. The lipophilicity value of compound **2C** also shows the permeability capacity. As seen in the Table S3, human hERG channel inhibition (pK_i) value of compound **2C** was determined to be −0.27, suggesting that compound **2C** may not play a role as hERG channel blocker; thus, its cardiotoxicity risks (i.e., long QT syndrome) will be limited. However, the predicted human serum protein binding percentage basaed on QSAR is found to be high, suggesting that compound **2C** can achieve effective drug concentrations and is very informative in establishing safety margins.

Compound 2C Inhibits Cell Proliferation and Colony Formation of Breast Cancer Cells. The effect of compound **2C** on cell proliferation and colony formation was evaluated in various breast cancer cell lines, including highly aggressive and invasive TNBC cells such as MDA-MB-231 (p53- and Kras-mutated), BT-20 (PI3K- and p53-mutated), and MDA-MB-436 (p53- and BRCA1-mutated) and noninvasive MCF-7 (ER$^+$) cells.[14] As shown in Figure 2A, treatment with the compound **2C** dramatically reduced cell proliferation and colony formation in breast cancer cell lines (Figure 2A). Compound **2C** inhibited cell proliferation and the number of colonies in at 1 μM or lower concentrations in most of the cell lines compared to DMSO treated control cells while previously published A484954 did not inhibit cell proliferation up to 50 μM drug concentrations in MDA-MB-231, MDA-MB-436, and BT-20 cells (Figure 2C−E). We also investigated the effect of **2C** on normal breast epithelial cells. The results showed that compound **2C** did not have any effect on a normal immortalized human mammary epithelial cell line (MCF-10A) (Figure 2E,F).

To demonstrate the role of eEF-2K in the proliferation and survival of breast cancer cells that were used for evaluation of the activity of the inhibitor compounds, we knocked down eEF-2K in MDA-MB-231, MDA-MB-436, and BT-20 cells by using a specific siRNA targeting eEF-2K mRNA.[13] As shown in Figure 2H, inhibition of eEF-2K by siRNA (50 nM) suppressed cell proliferation and colony formation of MDA-MB-436, BT-20, and MDA-MB-231 cells compared with control-siRNA treated cells. eEF-2K knockdown by eEF-2K

https://doi.org/10.1021/acsptsci.1c00030
ACS Pharmacol. Transl. Sci. 2021, 4, 926−940

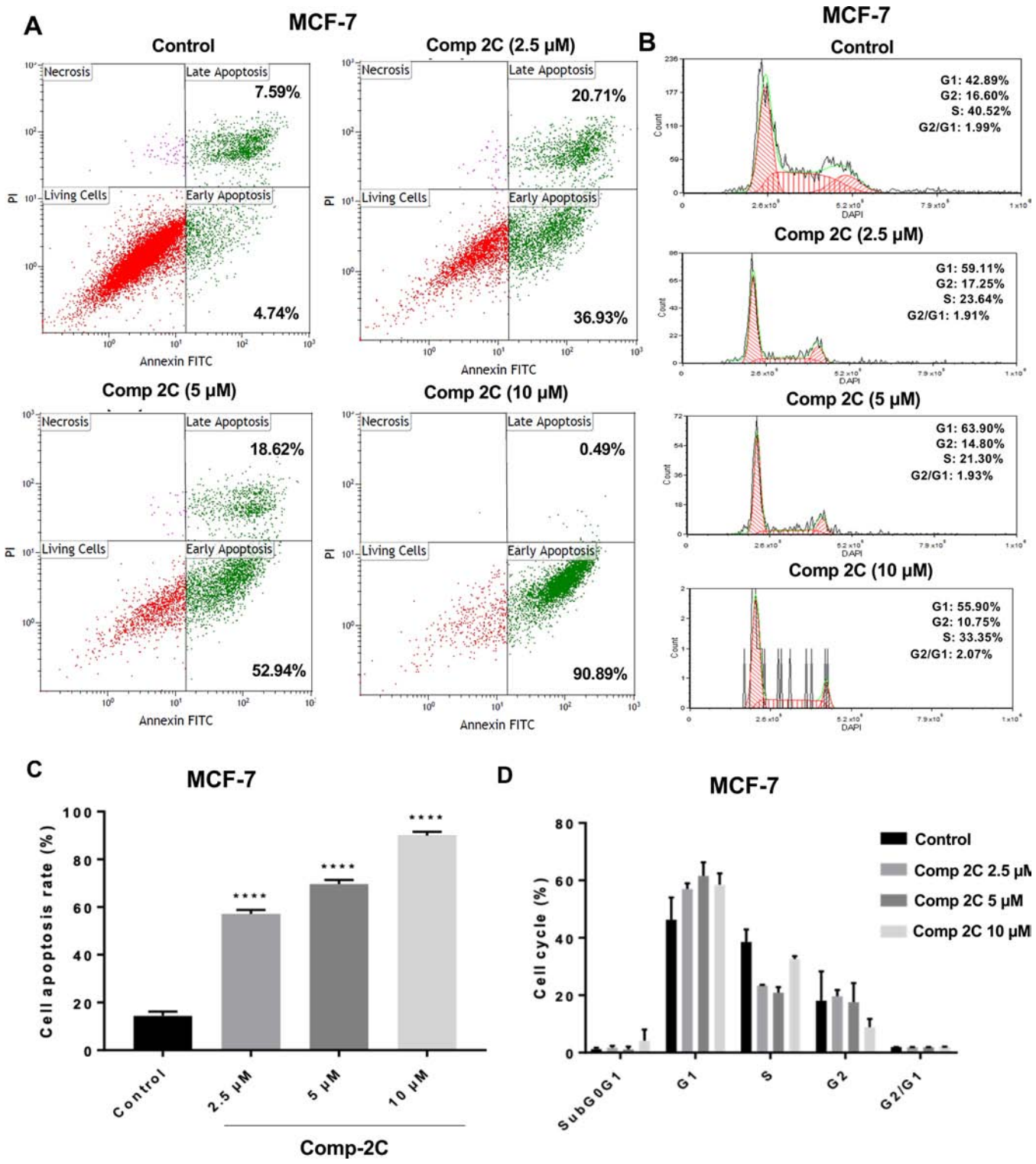

Figure 4. eEF-2K inhibitor compound **2C** induces apoptosis in ER+ breast cancer cells Compound **2C** induces apoptosis in MCF-7 cells. (A) MCF-7 cells were treated with compound **2C** (2.5−10 μM) for 72 h or left untreated and analyzed by PI staining and FACS. (B) Effect of compound **2C** on cell cycle distribution in breast cancer cells. MCF-7 cells were treated with compound **2C** and cell cycle was evaluated by FACS. (C, D) Bar graphs show the percentages of the cell apoptosis and cell cycle for MCF-7 cells.

siRNA was demonstrated in MDA-MB-436 through Western blot analysis (Figure 2I). For this purpose, MDA-MB-436 cells were transfected with eEF-2K or control siRNA (50 nM) and collected and analyzed 72 h later by Western blot. eEF-2K inhibition by siRNA reduced both EF2K and its downstream substrate p-EF2 (Thr56) levels in MDA-MB-436 cells

Compound 2C Inhibits eEF-2K Activity in Breast Cancer Cells. To determine the effect of **2C** on eEF-2K activity in breast cancer cells, we treated cells and evaluated the inhibition of eEF-2K by examiming p-EF2 (Thr56) levels by Western blot.[13,14] Treatment with compound **2C** led to a marked inhibition of eEF-2K as indicated by reduced levels of

https://doi.org/10.1021/acsptsci.1c00030
ACS Pharmacol. Transl. Sci. 2021, 4, 926−940

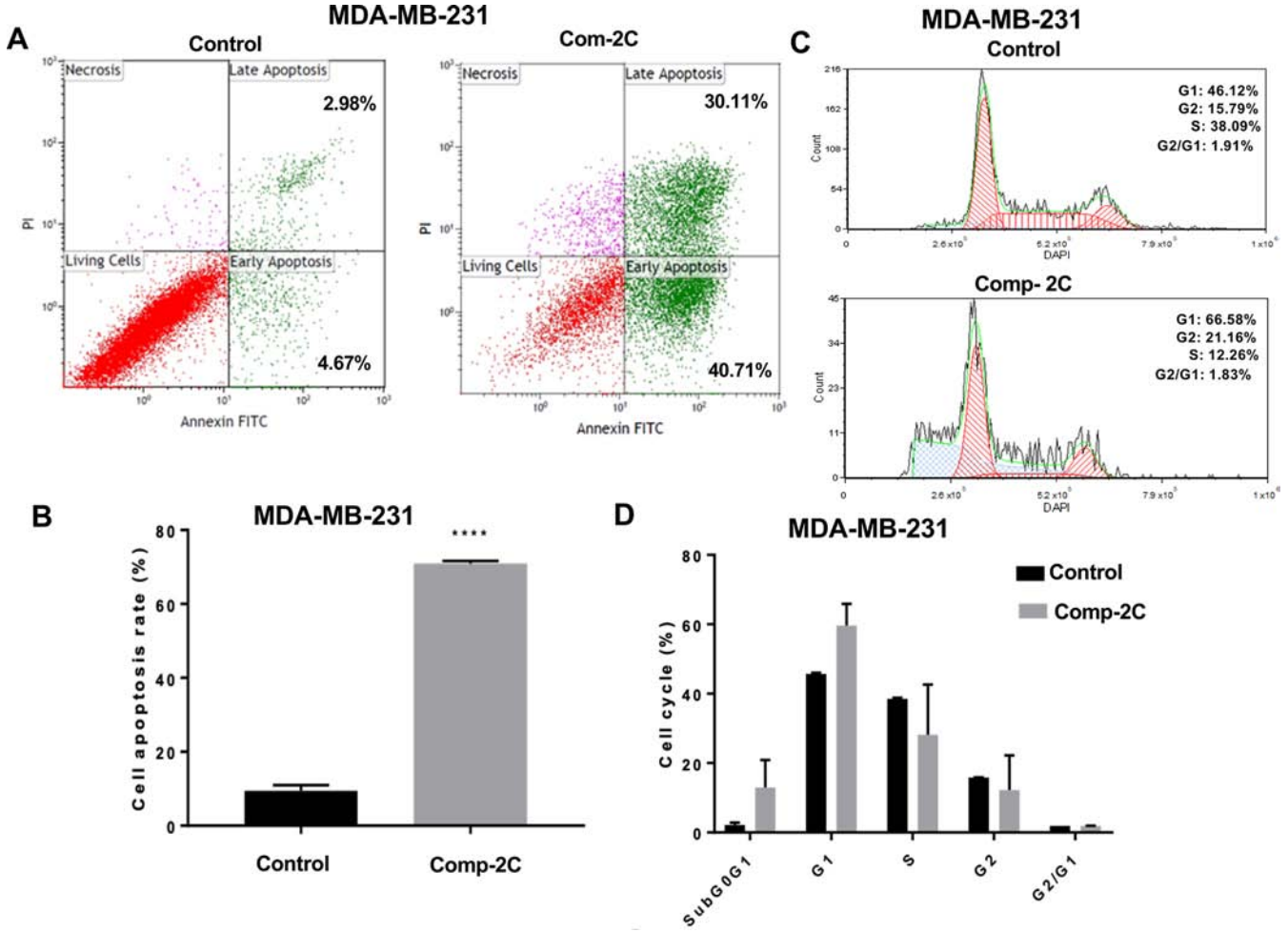

Figure 5. eEF-2K inhibitor compound **2C** induces apoptosis in TNBC cells. (A) MDA-MB-231 cells were treated with compound **2C** at 10 μM for 72 h. Annexin V-FITC and PI staining assay was used to determine the apoptotic cell death. (B) Levels of cell apoptosis showed a significant difference in the cells compared to DMSO. (C) Cell cycle was evaluated by FACS. (D) Bar graphs show the percentages of cell cycle for MDA-MB-231 cells.

p-EF2, a direct downstream target of eEF-2K, at 1 μM in breast cancer cells up to 48 h. GAPDH and β-actin were used as loading controls. Compound **2C** showed strong inhibition against eEF-2K at 0.1 μM (Figure 3A). Compound **2C** treatment inhibited eEF-2K in a dose-dependent manner at increasing doses (1, 2.5, and 5 μM) at 6 h (Figure 3B). The time-dependent inhibition of eEF-2K by compound **2C** (1 μM) was evaluated in TNBC MDA-MB-231 and ER$^+$ MCF-7 cells (Figure 3C,D). Our results indicated that inhibition of eEF-2K as indicated by reduced p-EF2 (Thr56) levels lasted up to 48 h (Figure 3C,D).

Compound 2C Induces Apoptosis and Alters Cell Cycle Distribution in Human Breast Cancer Cells. To evaluate of programmed cell death following the treatment of compound **2C** (2.5, 5, and 10 μM for 72 h) in breast cancer cells, we first investigated the induction of apoptosis by Annexin V-FITC and PI staining assay staining. These results revealed that compound **2C** induces apoptosis in all breast cancer cell lines. Compound **2C** induced dramatic increase in apoptotic cells in MCF-7 cells, leading to total number of late and early apoptotic cells percentage as high as 91.38% at the highest dose (Figures 4A,B). Compound **2C** significantly induced apoptosis in 70.8% of MDA-MB-231 cells compared to that in control treated cells (Figure 5A, 5B). MDA-MB-436 and BT20 cells underwent apoptotosis by **2C** treatment; however, the number of apoptotic cells was much lower compared to that in MCF7 cells (Figures 6A,B and 7A,B). To evaluate the mechanism by which **2C** inhibits cell proliferation, breast cancer cells were treated with **2C** and analyzed by cell cycle distribution and flow cytometry. Results showed significant accumulation in G1 and G2 and reduced SM phases following treatment with compound **2C** (Figures 4C,D−7C,D).

***In Vivo* Systemic Administration of the eEF-2k Inhibitor Encapsulated in Lipid Nanoparticles Suppresses Growth of Orthotopic Tumor Xenografts in TNBC Tumors in Mice.** To determine the *in vivo* eEF-2K inhibitory effect and therapeutic efficacy of compound **2C** in highly aggressive TNBC tumor models, MDA-MB-231 cells were orthotopically implanted into the mammary fat pad in nude mice. About 2 weeks later, single-lipid nanoparticles (SLNPs) incorporating **2C** (5 mice/group) were intraperitoneally (i.p.) administered twice a week at 20 mg/kg dose for 4 weeks. Because **2C** is a highly hydrophobic molecular not water-soluble, *in vivo* administration of **2C** we used SLNPs.[14,17,18] Liposomal NPs are commonly used due to their safety and increased payload delivery into tumor tissues because of the leaky nature of the angiogenic vessel

https://doi.org/10.1021/acsptsci.1c00030
ACS Pharmacol. Transl. Sci. 2021, 4, 926−940

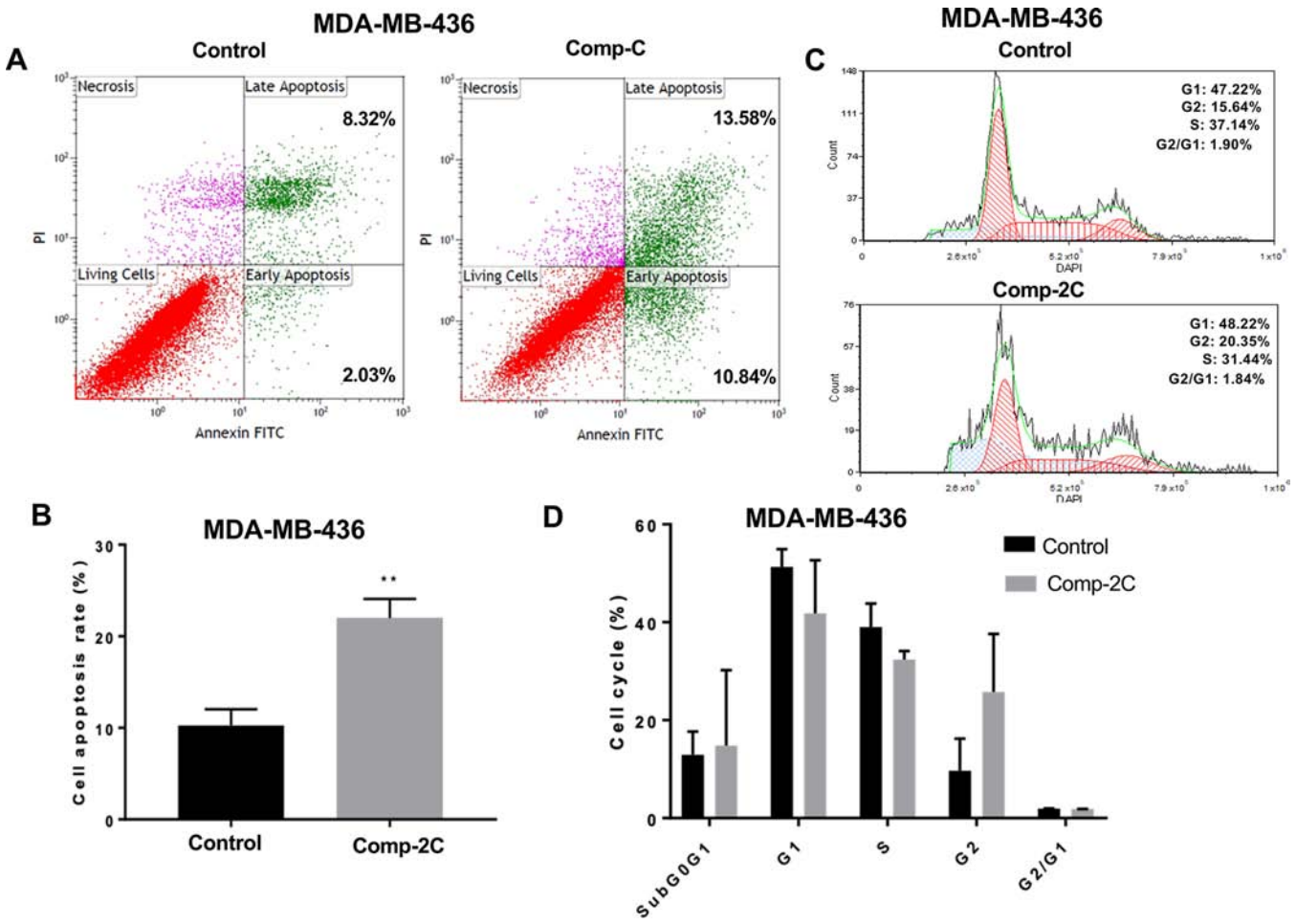

Figure 6. eEF-2K inhibitor compound **2C** induces apoptosis in TNBC cells. (A) MDA-MB-436 cells were treated with compound **2C** for 72 h. Annexin V-FITC and PI staining assay was used to determine the apoptotic cell death. (B) Levels of cell apoptosis showed a significant difference in the cells compared to DMSO. (C) Effect on cell cycle was evaluated by FACS. (D) Bar graphs show the percentages of cell cycle for MDA-MB-436 cells.

endothelium and increased junction gaps, reducing *in vivo* doses of drugs compared to free drugs. As shown in Figure 8A, treatment with SLNPs incorporating **2C** significantly inhibited tumor growth in mice ($p < 0.05$). Furthermore, we assessed the role of the inhibitor in inhibiting eEF-2K activity in *in vivo* TNBC tumors. As shown in Figure 8B, eEF-2K inhibitor treatment led to significant reduction in eEF-2K activity as indicated by reduced levels of p-EF2 (Thr56) in MDA-MB-231 tumor xenographs in mice by Western blot analysis compared to control treated tumors.

NP-2C Therapy Induces Apoptosis *In Vivo* in Breast Cancer Tumor Xenographs. Breast tumor cell apoptosis was assessed via immunofluorescent staining for TUNEL in tumors obtained in highly aggressive MDA-MB-231 tumor model. NP-**2C**-based therapy led to induction of significant apoptotic cell death in MDA-MB-231 tumors *in vivo* ($p = 0.014$) Figure 8C. Photomicrographs (magnification, 200×) of TUNEL-positive breast tumor cells (green) and tumor-cell nuclei (blue) (Figure 8C). The expression of Ki-67, an intratumoral proliferation marker, was visualized using IHC in breast tumor xenografts in mice after 4 weeks of treatment with 2C (Figure 8D) and quantified using densitometry with mean (±SD) values. Although there was a trend for inhibition of Ki-67, it was not statistically significant.

eEF-2K Inhibitor 2C Did Not Cause Any Toxicity in Mice. Treatment with eEF-2K inhibitor **2C** for 4 weeks did not cause any negative effects in eating habits of mice and behavioral change, appearance of mice nor did it lead to any observed toxicity. As shown in Figure 8E treatment with eEF-2K inhibitor NP-**2C** for 4 weeks did not cause weight loss in mice. Blood chemistry of toxicity markers for liver (i.e, ALP, AST, ALT, total bilurubin), kidneys (BUN, creatinine), total blood protein, globulin, albumin, and blood lipid lipids such as cholesterol were not markedly altered, suggesting that eEF-2K inhibitor **2C** is effective and safe for *in vivo* applications.

Compound 2C Is a Highly Potent Inhibitor of eEF-2K with Significant *In Vitro* and *In Vivo* Activity in Breast Cancer Models. The findings presented here suggest that compound **2C** is a highly potent inhibitor of eEF-2K with significant *in vitro* and *in vivo* activity in breast cancer models. Our results also demonstrated that compound **2C** binds to eEF-2K with high affinity, inhibits its activity at submicromolar concentrations and suppresses breast cancer proliferation. More importantly, *in vivo* treatment with compound **2C** encapsulated in SLNPs significantly suppressed growth of highly aggressive triple breast cancer tumor models in mice with no observed toxicity. Our results indicate that compound **2C** encapsulated in nanoliposomes is a highly effective approach for *in vivo* inhibition of eEF-2K and that **2C** may

https://doi.org/10.1021/acsptsci.1c00030
ACS Pharmacol. Transl. Sci. 2021, 4, 926−940

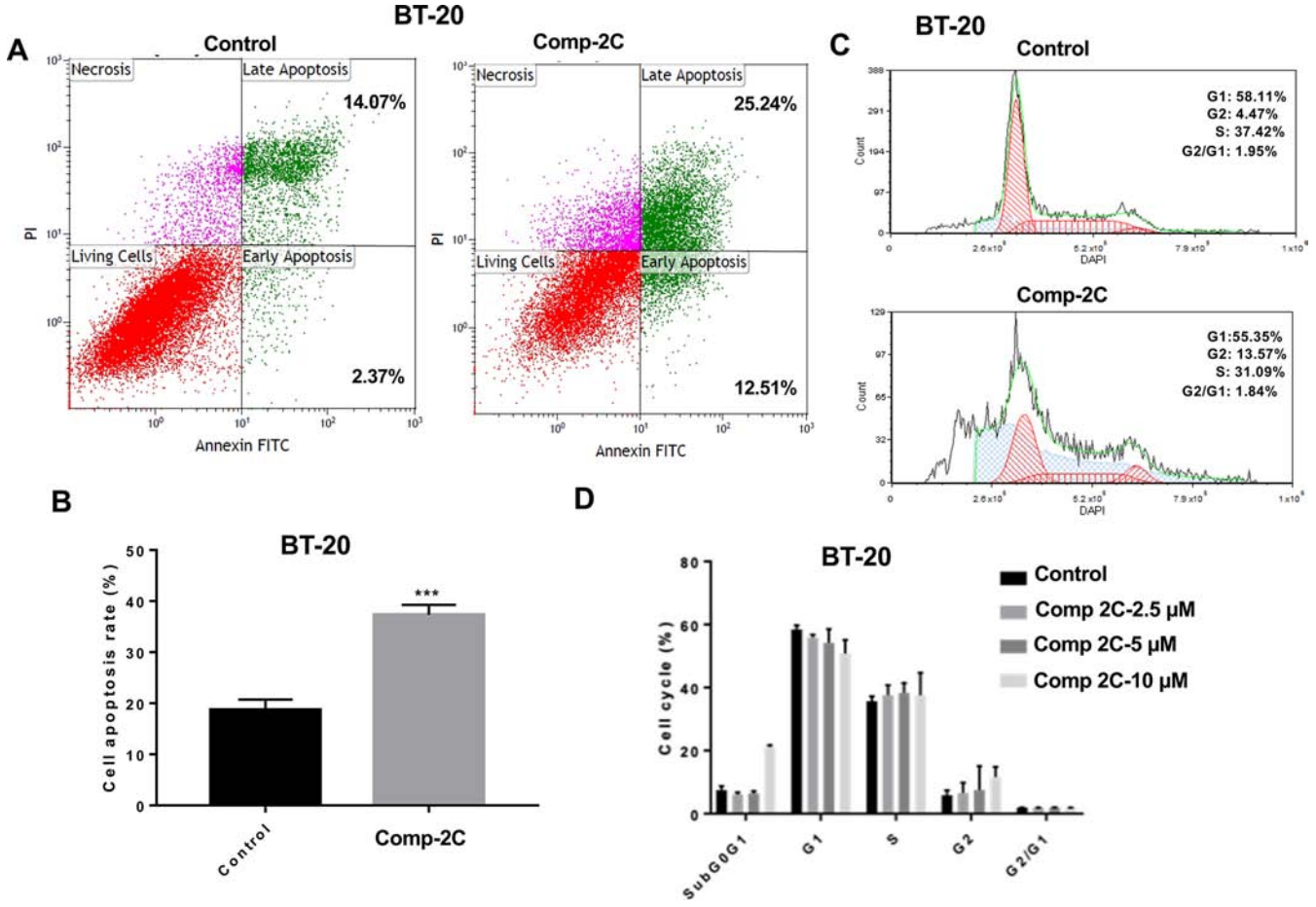

Figure 7. Compound **2C** induces apoptosis in BT-20 cells. (A) BT-20 cells were treated with compound **2C** for 72 h. Annexin V-FITC and PI staining assay was used to determine the apoptotic cell death. (B) Levels of cell apoptosis showed a significant difference in the cells compared to DMSO. (C) Effect on cell cycle was evaluated by FACS. (D) Bar graphs show the percentages of cell cycle for BT-20 cells.

be considered for further development of molecularly targeted therapies in breast and other cancers that overexpress eEF-2K and rely of this kinase for proliferation and survival.

Breast cancer is a heterogeneous disease with several major subtypes which harbor various growth factor receptors and mutations, leading to different clinical source and prognosis. TNBC is characterized by lack of molecular targets (e.g., ER, PR, and HER2 receptors) and considered an aggressive and metastatic subtype of breast cancer. TNBC tumors are treated with the conventional chemotherapies such as anthracyclines (e.g., doxorubicin) and taxane-based therapeutics quickly develop resistance to chemothrerapeutics and can not benefit from available targeted therapies including anti-estrogen hormone or HER2-targeted antibody therapies. Currently, there is no FDA-approved targeted therapy for TNBC patients. Identification of new molecular targets and potent inhibitor of these targets are critical for development of novel targeted treatments in TNBC to improve poor prognosis and dismal patient survival and reduce high mortality rates. Recently, using genetic methods, we have previously validated eEF-2K as a potential molecular target TNBC[13,14,19] pancreatic[15,16] and lung cancer.[17]

Highly potent and effective small-molecule inhibitors targeting eEF-2K are greatly needed for clinical translation and targeting of cancers that rely of eEF-2K for tumor growth and progression. In the current study, we discovered that coumarin−chalcone compounds may be potent and new inhibitors for eEF-2K and can be used for the purpose of developing clinically applicable targeted therapies. One of the major advantages of coumarins is that they are associated with low toxicity.[51] Chalcones are linked by a α,β-unsaturated carbonyl system.[37] Interestingly, one of the chalcones (i.e, rottlerin, a natural compound) has been reported act as a nonspecific eEF-2K inhibitor and inhibits various other protein kinases at concentrations lower than those needed to inhibit eEF-2K.[16,28] In the present study, we found that the presence of a CF_3 group at position 3 on the phenyl ring of the coumarinyl chalcone structure enhanced its eEF-2K inhibitor activity due to its electron withdrawing group properties and inductive effects of trifluoromethyl group.

NH125 has been reported to be the first eEF-2K inhibitor in the literature. However, we and others demonstrated that it acts as a nonspecific protein-aggregating agent.[29,30] A-484954 is a weak inhibitor of eEF-2K and has effective concentrations higher than 50−75 μM in cells. Another compound, a pyrido [2,3-*b*]pyrimidine-2,4-dione derivative, has been reported but is not more potent than A-484954; each only caused partial inhibition of eEF2 phosphorylation at 75 μM in MDA-MB-231 breast cancer cells.[52] Additionally, we have shown that a natural compound thymoquinone (TQ) inhibits eEF-2K and decrease the phosphorylation of EF2 and the expression of eEF-2K in a dose-dependent manner at 5 μM in breast cancer cells.[53] Although TQ was highly effective in inhibiting eEF-2K in *in vivo* tumor models at 20 mg/kg doses, it is not a specific

https://doi.org/10.1021/acsptsci.1c00030
ACS Pharmacol. Transl. Sci. 2021, 4, 926−940

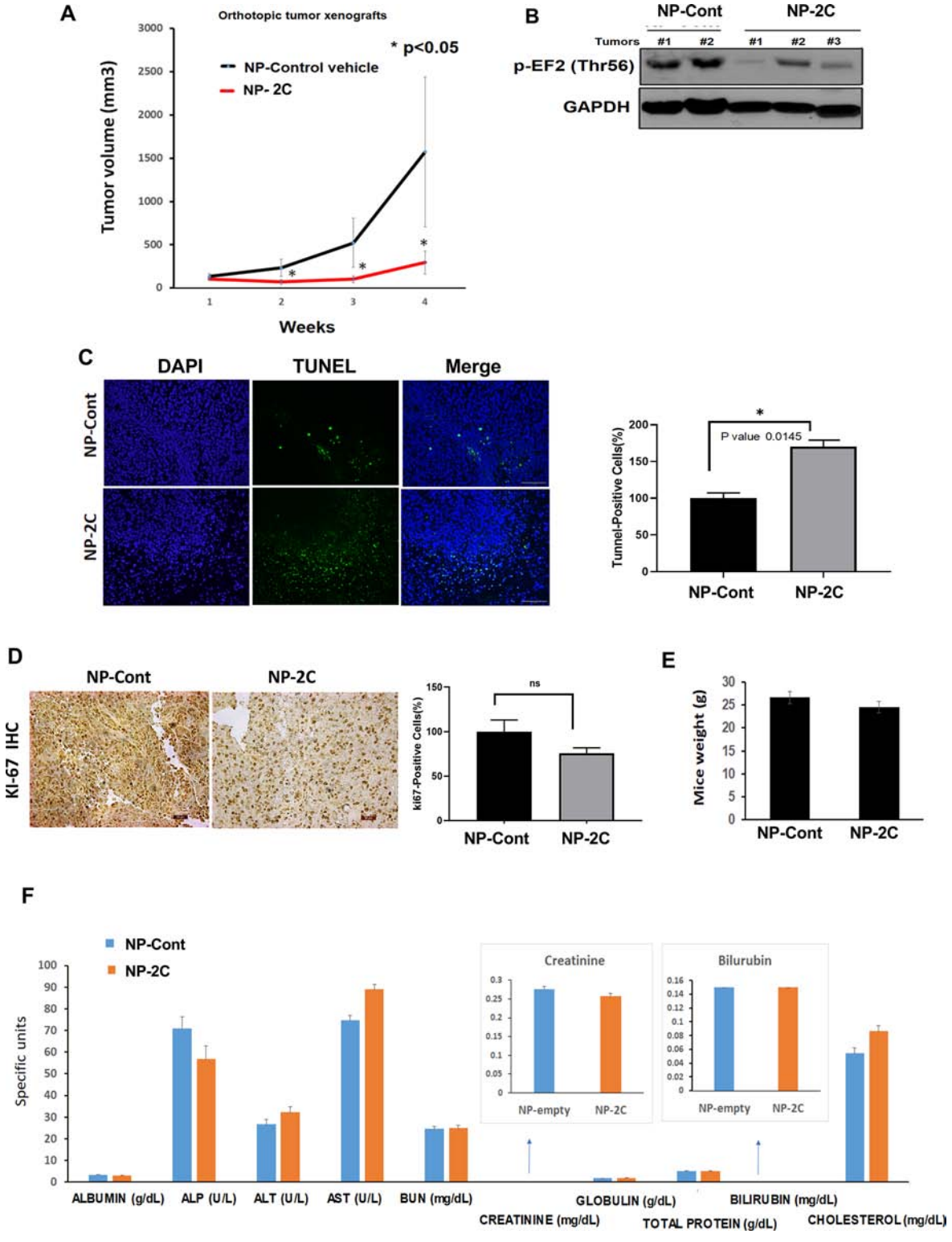

Figure 8. *In vivo* treatment with eEF-2K inhibitor 2C suppressed growth of highly aggressive MDA MB-231 tumors in orthotopic xenograph models in mice. (A) The mice were systemically treated with either SLNPs incorporating compound **2C** (20 mg/kg) or empty control nanoparticles. Tumor volumes were measured weekly by electronic calipers and are shown as mean ± SD. (B) Tumor samples from mice were collected 24 h after the last NP-**2C** or NP-control (empty vehicle) treatment and analyzed for pEF2 expression by Western blot. GAPDH was used as a loading control. (C, D) Immunohistochemical staining was used to evaluate the expression of *in vivo* apoptosis marker TUNEL and proliferation marker Ki-67, microvessel density marker CD31, and in MDA-MB-231 mouse xenografts treated with NP-**2C** or control NP-mimic. Positively stained cells in both treatment groups were quantified (lower panel) (scale bar = 100 nm). (E) Mice weights were measured after 4 weeks of NL-empty and NL-**2C** treatment. (F) Blood chemistry for toxicity markers were evaluated in serum after 4 weeks of NL-empty and NL-**2C** treatment.

https://doi.org/10.1021/acsptsci.1c00030
ACS Pharmacol. Transl. Sci. 2021, 4, 926−940

inhibitor of eEF-2K and inhibits other targets as well, making it difficult use in clinical settings.

The efforts for developing potent eEF-2K inhibitors have been hindered by the lack of a crystal and a 3D structure for eEF-2K. However, the development of a homology model of eEF-2K based on the known structures of other members of the α-kinase family such as CMAK has markedly increased rationale drug design and the discovery of potent and selective eEF-2K inhibitors.[47] In fact, using the homology modeling of eEF-2K using the homology modeling, we recently identified coumarin-3-carboxamides (A1 and A2) with morpholine and *tert*-butyl piperazine-1-carboxylate groups attached to the phenyl ring via the methylene bridge as eEF-2K inhibitors at 1 and 2.5 μM doses, respectively.[47] Here, we identified as one of the most effective eEF-2K inhibitors (compound **2C**) that is about 100-fold more potent and exerts a higher eEF-2K inhibitory activity compared with known eEF-2K inhibitors (i.e., A-484954, IC_{50} for cell proliferation = 75 μM).[31,32] More importantly, compound **2C** was very effective in inhibiting tumor growth of highly aggressive MDA-MB-231 TNBC model in mice at a 20 mg/kg twice a week injection with no observed toxicity, suggesting that **2C** may have a potential for *in vivo* applications.

The topology of the binding pocket region of the protein−ligand complex is largely dependent on conformational changes caused by the bound ligand. Unfortunately, unraveling the X-ray structure of a protein−ligand complex requires considerable time and investment and mostly is difficult. Since the IFD approach takes into account the flexibility of both the ligand and the active site residues, with this method it is possible to explore binding modes and associated conformational changes of both the docked ligand and crucial residues at the binding. Since the correct partial charges of ligand are crucial in docking, we carried out quantum mechanics calculations and used these charges at the docking site. eEF-2K does not have a deep binding pocket, so we used the top 5 docking poses of compound **2C** and carried out all-atom MD simulations for these poses. Results showed that two of the top five poses (poses 2 and 4) of **2C** have stable conformations and do not diffuse from the binding pocket and construct interactions with crucial residues. These two poses have similar binding modes with a slight difference in conformation, suggesting that data regarding interaction of **2C** with eEF-2K is highly reliable.

In conclusion, development of *in vivo* active and potent inhibitors targeting eEF-2K is greatly needed for clinical translation for cancer patients. Our findings indicate that compound **2C** is a potent, highly selective, *in vivo* active, and safe inhibitor of eEF-2K with no observed toxicity and induces significant apoptotic response in breast cancer tumors, suggesting that compound **2C** may be a potential therapeutic strategy for molecularly targeted strategies in breast cancer. Compound **2C** may be used as a therapeutic agent not only against breast cancer but also for other cancers such as lung and pancreatic cancers that are sensitive to eEF-2K inhibition. Further studies including extensive safety and pharmacokinetics studies need to be carried out for further development of this compound and completion of preclinical development.

MATERIALS AND METHODS

***In Silico* Pharmacokinetic Profiles of Compound 2C.** To investigate the *in silico* pharmacokinetic profiles of compound **2C**, the MetaCore/MetaDrug platform from Clarivate Analytics was used.[50] MetaCore/MetaDrug uses binary QSAR models for the prediction of the pharmacokinetic properties. The prediction of a therapeutic activity or toxic effect using recursive partitioning algorithm is calculated based on the ChemTree ability to correlate structural descriptors to that property. These pharmacokinetic properties successfully investigated the predicted toxicity and adsorption, distribution, metabolism, and excretion (ADME) of compound **2C**.

Molecular Modeling Studies. *Ligand Preparation.* Compound **2C** was prepared with the OPLS3 force field using LigPrep module (Schrodinger Release 2015−2, LigPrep) of the Maestro molecular modeling program. The protonation states at neutral pH 7 was determined by the Epik module.[54] Prepared ligands were further optimized by the quantum mechanics (QM) method using the Jaguar module of Maestro. For this aim, 6-31G* basis set, B3LYP density functional, and "ultrafine" SCF accuracy level was used. Mulliken partial charges were recorded, and these partial charges were used in further docking studies.

Protein Preparation. A model 3D structure of protein was used as a target. Protein Data Bank protein ID 5DYJ was used as a template to produce the 3D structure of the target protein. Homology modeling studies were carried out with Swiss Model. The target protein was prepared with the Protein Preparation module of Maestro. The protonation states of the residues were estimated in PROPKA at blood pH (7.4). Then, the refinement of protein coordinates with geometry optimization using the OPLS3 force field was carried out.[55]

Docking Studies Were Performed with Extended IFD Simulations. For rigid docking, we have used Autodock 4.2. The docking procedure used a rigid protein,[42] and a flexible ligand was identified with the Lamanckian genetic algorithm. The grid was adjusted to points 126, 126, and 126 in *x*-, *y*-, and *z*-directions with a grid spacing of 0.375 Å, and a distance-dependent function of the dielectric constant was used to calculate the energetic map. For flexible docking, we carried out IFD; thus, initially, Glide/SP was carried out. In geometry optimization, 5.0 Å around the docking poses was used. The refined binding pocket of the target protein[55] was then used in the redocking procedure using the Glide/XP protocol.[45−38] In QPLD calculations, initially Glide/SP docking was carried out to generate 10 poses for each docked compound. These poses were submitted to QM charge calculations which uses the 6-31G*/LACVP* basis set, B3LYP density functional, and "Ultrafine" SCF accuracy level.

Molecular Dynamics (MD) Simulations. The docking poses were used in MD simulations as input coordinates. TIP3P water models were used in solvation with 10.0 Å from the edges of protein for the determination of the solvation box. For MD simulations, the Desmond program was used. An MD protocol similar to that in our previously reported studies was used.[47] The last 50% of the trajectories from the MD simulations were used in free energy calculations. For this aim, MM/GBSA calculations from Prime were carried out.[39,40]

Synthesis of Compound 2C. A conventional synthesis method was applied to obtain 3-((*E*)-3-(3-(trifluoromethyl)-phenyl)acryloyl)-2*H*-chromen-2-one) (compound **2C**). For this purpose, 3-acetylcoumarin was synthesized with a high yield by Knoevenagel condensation reaction of salicylaldehyde and ethylacetoacetate using piperidine in ethanol under reflux.[43−41] This condensation method was used in the second step to obtain substituted coumarinyl chalcone in *n*-butanol as a solvent.[43,44]

https://doi.org/10.1021/acsptsci.1c00030
ACS Pharmacol. Transl. Sci. 2021, 4, 926−940

Cell Lines and Reagents. American Type Culture Collection (ATCC) (Manassas, VA) provided all cell lines including human highly aggressive and invasive triple-negative breast cancer (TNBC) cell lines (ER^-, PR^-, and $HER2^-$) such as MDA-MB-231, MDA-MB-436, and BT-20, and noninvazive estrogen receptor positive (ER^+) MCF-7 BC cells. Dulbecco's modified Eagle's medium (DMEM)/F12 was used for *in vitro* culture of TNBC, and MCF-7 cells were cultured with supplements such as 10% FBS and 1% penicillin−streptomycin.[54]

Cell Proliferation and Colony Formation Assay. Colony formation in the cells was detected with compound **2C**, and clonogenic assay was carried out according to our previous study.[47,53] For this purpose, breast cancer cells (300 cells/well) were seeded in 24-well plates and treated with changing doses of compound **2C** (1, 2.5, 5, and 10 μM and at decreased doses (0.1−1 μM)) and cultured for 8−12 days. Crystal violet was used to stain the colonies, and these were quantified using ImageJ software (National Institutes of Health, Bethesda, MD).

Protein Extraction and Western Blotting. Western blot analysis was carried out according to our previously reported studies.[16,53] Following the treatment of MDA-MB-231 cells with compound **2C**, primary antibodies including p-EF2 (Thr56), eEF2, eEF2K, and β-actin (Sigma) and their secondary antibodies were used to detect the expression levels. Time−response manner studies were carried out for compound **2C** in MDA-MB-231, MCF-7 cells at 1 μM concentration from times of 30 min to 48 h compared to DMSO. The most effective p-EF2 inhibition dose was determined. Finally, the time−response approach was applied to compound **2C** in MCF-7 cell lines. Cell signaling technology antibodies were used in this study.

Analysis of Cell Death and Cell Cycle. To determine programmed cell death levels, Annexin V assay was used as reported previously.[16] Cells were seeded in 25 cm^2 culture flasks (2×10^5 cells/flask). The cells were treated with increasing concentrations of potent compound **2C** (2.5, 5, and 10 μM) in TNBC cells for 72 h and cells treated with DMSO were used as a control. Annexin V/propidium iodide (PI) staining assay was applied to analyze the cells according to the manufacturer's protocol (BD Pharmingen FITC−Annexin V kit, San Diego, CA). FACS analysis was carried out to detect and quantified positive cells.

Orthotopic Xenograft Tumor Model of TNBC. MDA-MB-231 cells (2×10^6 cells in 20% matrigel) were injected into the mammary fat pad of each mouse and about 2 weeks later, SLNPs incorporating the eEF-2K inhibitor compound **2C** was administered twice a week, at two different doses (20 mg/kg) by intravenous injection. Nanoparticles incorporating eEF-2K inhibitor were prepared based on a method previously published by us.[53] Tumor volumes were evaluated weekly by electronic calipers. After 4 weeks of treatment and 24 h after the last injection, mice were euthanized under constant CO_2, and tumors were removed and kept at −80 °C. Later, tumor tissues were lysed and analyzed by Western blot for evaluation of p-EF2 and eEF-2K inhibition.

Evaluation of apoptosis by TUNEL (TdT-Mediated dUTP Nick End Labeling) Assay. Apoptotic events after treatment with liposomal siRNA and/or chemotherapy regimens were determined by the TdT-mediated dUTP nick end labeling (TUNEL) assay (Promega, Madison, WI) in tumor sections, according to the manufacturer's protocol as described previously.[13]

Immunohistochemistry. Tumor samples of MDA-MB-231 tumors were obtained from the mice, and formalin-fixed and paraffin-embedded tumors were sectioned (5 μm) and stained with hematoxylin and eosin. Immunostaining for Ki-67 was carried out to evaluate intratumoral cell proliferation according to the manufacturer's protocol. After staining, slides were analyzed under an Eclipse TE200-U microscope (Nikon Instruments Inc., Melville, NY) as previously described.[14]

***In Vivo* Preliminary Toxicity of SLNP-EF2K Inhibitor (2C) in Mice.** eEF-2K inhibitor (**2C**)-incorporating SLNP nanoliposomes (n = 5 mice) or empty SLNP (control, n = 5 mice) were intravenously injected (20 mg/kg) into the tail of mice in 100 μL of PBS, and 48 h of later blood samples were collected. Biochemical toxicity markers were evaluated as follows: kidney (BUN, creatinine), liver (ASL, ALT, ALKP), and lipid panel (lipid, triglceride), Albumin, globulin, and blood organ toxicity marker (LDH) were evaluated in serum.

Statistical Analysis. Data of three independent experiments was given as mean ± SD. Student's t-test was used for statistical analysis. P values less than 0.05 were considered statistically significant and are indicated by an asterisk.

■ ASSOCIATED CONTENT

Supporting Information

The Supporting Information is available free of charge at https://pubs.acs.org/doi/10.1021/acsptsci.1c00030.

Interaction analysis of homology model of eEF-2K with compound **2C**, RMSD-time plot of protein and top and second top-poses of **2C**, QPLD docking score comparison of **2C** with other eEF-2K inhibitors, IFD docking score comparison of **2C** at the clinically important kinases, and Predicted ADME profiles of the compound **2C** (PDF)

■ AUTHOR INFORMATION

Corresponding Authors

Bulent Ozpolat − *Department of Experimental Therapeutics and Center for RNA Interference and Non-Coding RNAs, The University of Texas, MD Anderson Cancer Center, Houston, Texas 77030, United States;* orcid.org/0000-0003-1190-9255; Email: bozpolat@mdanderson.org

Mehmet Ay − *Department of Chemistry, Natural Products and Drug Research Laboratory, Faculty of Science and Arts, Çanakkale Onsekiz Mart University, 17020 Canakkale, Turkey;* orcid.org/0000-0002-1095-1614; Email: mehmetay06@comu.edu.tr

Authors

Ferah Comert Onder − *Department of Experimental Therapeutics, The University of Texas, MD Anderson Cancer Center, Houston, Texas 77030, United States; Department of Medical Biology, Çanakkale Onsekiz Mart University, Faculty of Medicine, 17020 Canakkale, Turkey; Department of Chemistry, Natural Products and Drug Research Laboratory, Faculty of Science and Arts, Çanakkale Onsekiz Mart University, 17020 Canakkale, Turkey*

Nermin Kahraman − *Department of Experimental Therapeutics, The University of Texas, MD Anderson Cancer Center, Houston, Texas 77030, United States*

https://doi.org/10.1021/acsptsci.1c00030
ACS Pharmacol. Transl. Sci. 2021, 4, 926−940

Esen Bellur Atici − *DEVA Holding A.S. Cerkezkoy, 59500 Tekirdag, Turkey*
Ali Cagir − *Izmir Institute of Technology, Department of Chemistry, Bioorganic and Medicinal Chemistry Laboratory, 35430 Urla, Turkey*
Hakan Kandemir − *Tekirdag Namik Kemal University, Department of Chemistry, 59030 Tekirdag, Turkey*
Gizem Tatar − *Gaziantep University, Institute of Health Sciences, Department of Bioinformatics and Computational Biology, 27310 Gaziantep, Turkey*
Tugba Taskin Tok − *Gaziantep University, Institute of Health Sciences, Department of Bioinformatics and Computational Biology, 27310 Gaziantep, Turkey; Gaziantep University, Faculty of Arts and Sciences, Department of Chemistry, 27310 Gaziantep, Turkey*
Goknur Kara − *Department of Experimental Therapeutics, The University of Texas, MD Anderson Cancer Center, Houston, Texas 77030, United States*
Bekir Karliga − *DEVA Holding A.S. Cerkezkoy, 59500 Tekirdag, Turkey*
Serdar Durdagi − *Department of Biophysics, School of Medicine, Computational Biology and Molecular Simulations Laboratory, Bahcesehir University, 34734 Istanbul, Turkey;* orcid.org/0000-0002-0426-0905

Complete contact information is available at: https://pubs.acs.org/10.1021/acsptsci.1c00030

Funding

This study was funded by The Scientific and Technological Research Council of Turkey (TUBITAK) (grant number 215S008 and TUBITAK-BIDEB 2214A program, F.C.O.) and The University of Texas-MD Anderson Cancer Center Bridge fund (B.O. and N.K.) and NIH-NCI 1R01CA244344 grants (B.O. and N.K.).

Notes

The authors have a pending patent application for compund **2C**.

Ethics Statement: Nude athymic female mice were obtained from MD Anderson Cancer Center, Department of Experimental Radiation Oncology Department. All *in vivo* studies were conducted according to the experimental protocol approved by the MD Anderson Institutional Animal Care and Use Committee.

The authors declare no competing financial interest.

REFERENCES

(1) Ryazanov, A. G., Shestakova, E. A., and Natapov, P. G. (1988) Phosphorylation of elongationfactor 2 by EF-2 kinase affects rate of translation. *Nature 334*, 170−173.
(2) Nairn, A. C., and Palfrey, H. C. (1987) Identification of the Major Mr 100,000 Substrate for Calmodulin-dependent Protein Kinase III in Mammalian Cells as Elongation Factor-2. *J. Biol. Chem. 262*, 17299−17303.
(3) Ryazanov, A. G., Ward, M. D., Mendola, C. E., Pavur, K. S., Dorovkov, M. V., Wiedmann, M., Erdjument-Bromage, H., Tempst, P., Parmer, T. G., Prostko, C. R., Germino, F. J., and Hait, W. N. (1997) Identification of a new class of protein kinases represented by eukaryotic elongation factor-2 kinase. *Proc. Natl. Acad. Sci. U. S. A. 94*, 4884−4889.
(4) Abramczyk, O., Tavares, C. D., Devkota, A. K., Ryazanov, A. G., Turk, B. E., Riggs, A. F., Ozpolat, B., and Dalby, K. N. (2011) Purification and characterization of tagless recombinant human elongation factor 2 kinase (eEF-2K) expressed in Escherichia coli. *Protein Expression Purif. 79*, 237−44.
(5) Tavares, C. D., O'Brien, J. P., Abramczyk, O., Devkota, A. K., Shores, K. S., Ferguson, S. B., Kaoud, T. S., Warthaka, M., Marshall, K. D., Keller, K. M., et al. (2012) Calcium/calmodulin stimulates the autophosphorylation of elongation factor 2 kinase on Thr-348 and Ser-500 to regulate its activity and calcium dependence. *Biochemistry 51*, 2232−2245.
(6) Parmer, T. G., Ward, M. D., Yurkow, E. J., Vyas, V. H., Kearney, T. J., and Hait, W. N. (1999) Activity and regulation by growth factors of calmodulin-dependent protein kinase III (elongation factor 2-kinase) in human breast cancer. *Br. J. Cancer 79*, 59−64.
(7) Horman, S., Browne, G., Krause, U., Patel, J., Vertommen, D., Bertrand, L., Lavoinne, A., Hue, L., Proud, C., and Rider, M. (2002) Activation of AMP-activated protein kinase leads to the phosphorylation of elongation factor 2 and an inhibition of protein synthesis. *Curr. Biol. 12*, 1419−23.
(8) Connolly, E., Braunstein, S., Formenti, S., and Schneider, R. J. (2006) Hypoxia inhibits protein synthesis through a 4E-BP1 and elongation factor 2 kinase pathway controlled by mTOR and uncoupled in breast cancer cells. *Mol. Cell. Biol. 26*, 3955−3965.
(9) Leprivier, G., Remke, M., Rotblat, B., Dubuc, A., Mateo, A. R., Kool, M., Agnihotri, S., El-Naggar, A., Yu, B., Prakash Somasekharan, S., et al. (2013) The eEF2 kinase confers resistance to nutrient deprivation by blocking translation elongation. *Cell 153*, 1064−1079.
(10) Usui, T., Okada, M., Hara, Y., and Yamawaki, H. (2013) Eukaryotic elongation factor 2 kinase regulates the development of hypertension through oxidative stress-dependent vascular inflammation. *Am. J. Physiol.Heart Circ. Physiol. 305*, H756−H68.
(11) Cheng, Y., Ren, X., Yuan, Y., Shan, Y., Li, L., Chen, X., Zhang, L., Takahashi, Y., Yang, J. W., Han, B., et al. (2016) eEF-2 kinase is a critical regulator of Warburg effect through controlling PP2A-A synthesis. *Oncogene 35*, 6293−6308.
(12) Lazarus, M. B., Levin, R. S., and Shokat, K. M. (2017) Discovery of new substrates of the elongation factor-2 kinase suggests a broader role in the cellular nutrient response. *Cell. Signalling 29*, 78−83.
(13) Tekedereli, I., Alpay, S. N., Tavares, C. D. J., Cobanoglu, Z. E., Kaoud, T. S., Sahin, I., Sood, A. K., Lopez-Berestein, G., Dalby, K. N., and Ozpolat, B. (2012) Targeted silencing of elongation factor 2 kinase suppresses growth and sensitizes tumors to doxorubicin in an orthotopic model of breast cancer. *PLoS One 7*, e41171.
(14) Bayraktar, R., Ivan, C., Bayraktar, E., Kanlikilicer, P., Kabil, N. N., Kahraman, N., Mokhlis, H. A., Karakas, D., Rodriguez-Aguayo, C., Arslan, A., et al. (2018) Dual suppressive effect of miR-34A on the FOXM1/EEF2-kinase axis regulates triple-negative breast cancer growth and invasion. *Clin. Cancer Res. 24*, 4225−4241.
(15) Ashour, A. A., Gurbuz, N., Alpay, S. N., Abdel-Aziz, A-A. H., Mansour, A. M., Huo, L., and Ozpolat, B. (2014) Elongation factor-2 kinase regulates TG2/β1 integrin/Src/uPAR pathway and epithelial-mesenchymal transition mediating pancreatic cancer cells invasion. *J. Cell. Mol. Med. 18*, 2235−2251.
(16) Ashour, A. A., Abdel-Aziz, A-A. H., Mansour, A. M., Alpay, S. N., Huo, L., and Ozpolat, B. (2014) Targeting elongation factor-2 kinase (eEF-2K) induces apoptosis in human pancreatic cancer cells. *Apoptosis 19*, 241−250.
(17) Bircan, H. A., Gurbuz, N., Pataer, A., Caner, A., Kahraman, N., Bayraktar, E., Bayraktar, R., Erdogan, M. A., Kabil, N., and Ozpolat, B. (2018) Elongation factor-2 kinase (eEF-2K) expression is associated with poor patient survival and promotes proliferation, invasion and tumor growth of lung cancer. *Lung cancer 124*, 31−39.
(18) Hamurcu, Z., Kahraman, N., Ashour, A., and Ozpolat, B. (2017) FOXM1 transcriptionally regulates expression of integrin β1 in triple-negative breast cancer. *Breast Cancer Res. Treat. 163*, 485−493.
(19) Asik, E., Akpinar, Y., Caner, A., Kahraman, N., Guray, T., Volkan, M., Albarracin, C., Pataer, A., Arun, B., and Ozpolat, B. (2019) EF2-kinase targeted cobalt-ferrite siRNA-nanotherapy suppresses BRCA1-mutated breast cancer. *Nanomedicine 14*, 2315−2338.
(20) Gschwendt, M., Horn, F., Kittstein, W., and Marks, F. (1983) Inhibition of the calcium- and phospholipid-dependent protein kinase

activity from mouse brain cytosol by quercetin. *Biochem. Biophys. Res. Commun. 117*, 444−447.
(21) Gschwendt, M., Horn, F., Kittstein, W., Fürstenberger, G., Besemfelder, E., and Marks, F. (1984) Calcium and phospholipid-dependent protein kinase activity in mouse epidermis cytosol. Stimulation by complete and incomplete tumor promoters and inhibition by various compounds. *Biochem. Biophys. Res. Commun. 124*, 63−68.
(22) Hidaka, H., Inagaki, M., Kawamoto, S., and Sasaki, Y. (1984) Isoquinolinesulfonamides, novel and potent inhibitors of cyclic nucleotide-dependent protein kinase and protein kinase C. *Biochemistry 23*, 5036−5041.
(23) Herbert, J. M., Augereau, J. M., Gleye, J., and Maffrand, J. P. (1990) Chelerythrine is a potent and specific inhibitor of protein kinase C. *Biochem. Biophys. Res. Commun. 172*, 993−999.
(24) Gschwendt, M., Leibersperger, H., Kittstein, W., and Marks, F. (1992) Protein kinase Cff and r/in murine epidermis TPA induces down-regulation of PKCr/but not PKC. *FEBS Lett. 307*, 151−155.
(25) Akiyama, T., Ishida, J., Nakagawa, S., Ogawara, H., Watanabe, S., Itoh, N., Shibuya, M., and Fukami, Y. (1987) Genistein, a specific inhibitor of tyrosine-specific protein kinases. *J. Biol. Chem. 262*, 5592−5595.
(26) Geissler, J. F., Traxler, P., Regenass, U., Murray, B. J., Roesel, J. L., Meyer, T., McGlynn, E., Storni, A., and Lydon, N. B. (1990) Thiazolidine-diones. Biochemical and biological activity of a novel class of tyrosine protein kinase inhibitors. *J. Biol. Chem. 265*, 22255−22261.
(27) Norman, J. A., Ansell, J., Stone, G. A., Wennogle, L. P., and Wasley, J. W. (1987) CGS 9343B, a Novel, Potent, and Selective Inhibitor of Calmodulin Activity. *Mol. Pharm. 31*, 535−540.
(28) Gschwendt, M., Kittstein, W., and Marks, F. (1994) Elongation factor-2 kinase: effective inhibition by the novel protein kinase inhibitor rottlerin and relative insensitivity towards staurosporine. *FEBS Lett. 338*, 85−88.
(29) Devkota, A. K., Tavares, C. D. J., Warthaka, M., Abramczyk, O., Marshall, K. D., Kaoud, T. S., Gorgulu, K., Ozpolat, B., and Dalby, K. N. (2012) Investigating the Kinetic Mechanism of Inhibition of Elongation Factor 2 Kinase by NH125: Evidence of a Common in Vitro Artifact. *Biochemistry 51*, 2100−2112.
(30) Chen, Z., Gopalakrishnan, S. M., Bui, M. H., Soni, N. B., Warrior, U., Johnson, E. F., Donnelly, J. B., and Glaser, K. B. (2011) 1-Benzyl-3-cetyl-2-methylimidazolium iodide (NH125) Induces Phosphorylation of Eukaryotic Elongation Factor-2 (eEF2). *J. Biol. Chem. 286*, 43951−43958.
(31) Edupuganti, R., Wang, Q., Tavares, C. D., Chitjian, C. A., Bachman, J. L., Ren, P., Anslyn, E. V., and Dalby, K. N. (2014) Synthesis and biological evaluation of pyrido[2,3-d]pyrimidine-2,4-dione derivatives as eEF-2K inhibitors. *Bioorg. Med. Chem. 22*, 4910−4916.
(32) Wang, X., Xie, J., Regufe da Mota, S., Moore, C. E., and Proud, C. G. (2015) Regulated stability of eukaryotic elongation factor 2 kinase requires intrinsic but not ongoing activity. *Biochem. J. 467*, 321−331.
(33) Hori, H., Nagasawa, H., Ishibashi, M., Uto, Y., Hirata, A., Saijo, K., Ohkura, K., Kirk, K. L., and Uehara, Y. (2002) TX-1123: An Antitumor 2-Hydroxyarylidene-4-cyclopentene-1,3-Dione as a Protein Tyrosine Kinase Inhibitor Having Low Mitochondrial Toxicity. *Bioorg. Med. Chem. 10*, 3257−3265.
(34) Devkota, A. K., Edupuganti, R., Yan, C., Shi, Y., Jose, J., Wang, Q., Kaoud, T. S., Cho, E. J., Ren, P., and Dalby, K. N. (2014) Reversible covalent inhibition of eEF-2K by carbonitriles. *ChemBioChem 15*, 2435−42.
(35) Comert Onder, F., Kahraman, N., Bellur Atici, E., Cagir, A., Kandemir, H., Tatar, G., Taskin Tok, T., Karliga, B., Durdagi, S., Ay, M., and Ozpolat, B. (November 8, 2020) Target-driven design of a coumarinyl chalcone scaffold based novel EF2 Kinase inhibitor suppresses breast cancer growth *in vivo*. *bioRxiv (Cancer Biology)*, 2020.11.06.371062, DOI: 10.1101/2020.11.06.371062.
(36) Tatar, G. (2018) Structure Prediction of Eukaryotic Elongation Factor 2 Kinase (eEF-2K) and Elucidation of Binding Mechanisms of its Novel Compounds with Molecular Modelling Applications, Ph.D Thesis, Gaziantep University.
(37) Comert Onder, F., Durdagi, S., Sahin, K., Ozpolat, B., and Ay, M. (2020) Design, Synthesis, and Molecular Modeling Studies of Novel Coumarin Carboxamide Derivatives as eEF-2K Inhibitors. *J. Chem. Inf. Model. 60*, 1766−1778.
(38) Frisch, M. J., Trucks, G. W., Schlegel, H. B., Scuseria, G. E., Robb, M. A., Cheeseman, J. R., Scalmani, G., Barone, V., Mennucci, B., Petersson, G. A., Nakatsuji, H., Caricato, M., Li, X., Hratchian, H. P., Izmaylov, A. F., Bloino, J., Zheng, G., Sonnenberg, J. L., Hada, M., Ehara, M., Toyota, K., Fukuda, R., Hasegawa, J., Ishida, M., Nakajima, T., Honda, Y., Kitao, O., Nakai, H., Vreven, T., Montgomery, J. A., Jr., Peralta, J. E., Ogliaro, F., Bearpark, M., Heyd, J. J., Brothers, E., Kudin, K. N., Staroverov, V. N., Kobayashi, R., Normand, J., Raghavachari, K., Rendell, A., Burant, J. C., Iyengar, S. S., Tomasi, J., Cossi, M., Rega, N., Millam, J. M., Klene, M., Knox, J. E., Cross, J. B., Bakken, V., Adamo, C., Jaramillo, J., Gomperts, R., Stratmann, R. E., Yazyev, O., Austin, A. J., Cammi, R., Pomelli, C., Ochterski, J. W., Martin, R. L., Morokuma, K., Zakrzewski, V. G., Voth, G. A., Salvador, P., Dannenberg, J. J., Dapprich, S., Daniels, A. D., Farkas, O., Foresman, J. B., Ortiz, J. V., Cioslowski, J., and Fox, D. J. (2009) *Gaussian 09*, revision E.01, Gaussian, Inc., Wallingford, CT.
(39) Fiser, A., and Šali, A. (2003) Modeller: Generation and Refinement of Homology-Based Protein Structure Models. *Methods Enzymol. 374*, 461−491.
(40) Morris, G. M., Huey, R., Lindstrom, W., Sanner, M. F., Belew, R. K., Goodsell, D. S., and Olson, A. J. (2009) AutoDock4 and AutoDockTools4: Automated Docking with Selective Receptor Flexibility. *J. Comput. Chem. 30*, 2785−2791.
(41) Is, Y. S., Durdagi, S., Aksoydan, B., and Yurtsever, M. (2018) Proposing Novel MAO-B Hit Inhibitors Using Multidimensional Molecular Modeling Approaches and Application of Binary QSAR Models for Prediction of Their Therapeutic Activity, Pharmacokinetic and Toxicity Properties. *ACS Chem. Neurosci. 9* (7), 1768−1782.
(42) Trivedi, J. C., Bariwal, J. B., Upadhyay, K. D., Naliapara, Y. T., Joshi, S. K., Pannecouque, C. C., De Clercq, E., and Shah, A. K. (2007) Improved and rapid synthesis of new coumarinyl chalcone derivatives and their antiviral activity. *Tetrahedron Lett. 48*, 8472−8474.
(43) Jayashree, B. S., Yusuf, S., and Kumar, D. V. (2009) Synthesis of Some Coumarinyl Chalcones of Pharmacological Interest. *Asian J. Chem. 21*, 5918−5922.
(44) Liu, R., and Proud, C. G. (2016) Eukaryotic elongation factor 2 kinase as a drug target in cancer, and in cardiovascular and neurodegenerative diseases. *Acta Pharmacol. Sin. 37*, 285−294.
(45) Kabil, N., Bayraktar, R., Kahraman, N., Mokhlis, H. A., Calin, G. A., Lopez-Berestein, G., and Ozpolat, B. (2018) Thymoquinone inhibits cell proliferation, migration, and invasion by regulating the elongation factor 2 kinase (eEF-2K) signaling axis in triple-negative breast cancer. *Breast Cancer Res. Treat. 171*, 593−605.
(46) Shelley, J. C., Cholleti, A., Frye, L. L., Greenwood, J. R., Timlin, M. R., and Uchimaya, M. (2007) A software program for pK(a) prediction and protonation state generation for drug-like molecules. *J. Comput.-Aided Mol. Des. 21*, 681−691.
(47) Madhavi Sastry, G., Adzhigirey, M., Day, T., Annabhimoju, R., and Sherman, W. (2013) Protein and ligand preparation: parameters, protocols, and influence on virtual screening enrichments. *J. Comput.-Aided Mol. Des. 27*, 221−234.
(48) Jorgensen, W. L., and Tirado-Rives, J. (1988) The OPLS Force Field for Proteins. Energy Minimizations for Crystals of Cyclic Peptides and Crambin. *J. Am. Chem. Soc. 110*, 1657−1666.
(49) Cho, A. E., Guallar, V., Berne, B. J., and Friesner, R. (2005) Importance of Accurate Charges in Molecular Docking: Quantum Mechanical/ Molecular Mechanical (QM/MM) Approach. *J. Comput. Chem. 26*, 915−931.

(50) Sherman, W., Day, T., Jacobson, M. P., Friesner, R. A., and Farid, R. (2006) Novel Procedure for Modeling Ligand/Receptor Induced Fit Effects. *J. Med. Chem. 49*, 534−553.
(51) D. E. Shaw Research. (2021) *Desmond Molecular Dynamics System*, Schrödinger, Inc., New York.
(52) Kanan, T., Kanan, D., Erol, I., Yazdi, S., Stein, M., and Durdagi, S. (2019) Targeting the NF-κB/IκBα complex via fragment-based E-Pharmacophore virtual screening and binary QSAR models. *J. Mol. Graphics Modell. 86*, 264−277.
(53) Qiang, D. z., Shi, J. B., Song, B. A., and Liu, X. H. (2014) Novel 2*H*-chromen derivatives: design, synthesis, and anticancer activity. *RSC Adv. 4*, 5607−5617.
(54) Ay, M., Ozpolat, B., Comert Onder, F., Taşkin Tok, T., Bellur Atici, E., Karliga, B., Kandemir, H., Cagir, A., Sahiner, N., and Tatar, G. (2019) EF2 Kinase Enzyme Inhibiting Novel Compounds. WO2019/240701 A1.
(55) Nageshwar, M., Ambica, D., Garlapati, A., and Ravikumar, M. (2017) Synthesis, characterization and antibacterial activity screening of some novel pyrazole derivative. *World J. Pharm. Sci. 6*, 2407−2417.

NOTE ADDED AFTER ASAP PUBLICATION

This paper was published ASAP on March 30, 2021, with the references incorrectly ordered. The corrected version was posted April 9, 2021.

https://doi.org/10.1021/acsptsci.1c00030
ACS Pharmacol. Transl. Sci. 2021, 4, 926−940